Nanostructured Thermosets from Epoxy Resin and an Organic−Inorganic Amphiphile

Yong Ni and Sixun Zheng*

Department of Polymer Science and Engineering, Shanghai Jiao Tong University, Shanghai 200240, P. R. China

Received April 22, 2007; Revised Manuscript Received July 19, 2007

ABSTRACT: Polyhedral oligomeric silsesquioxane (POSS)-capped PCL was synthesized via ring-opening polymerization of ϵ-caprolactone with 3-hydroxypropylheptaphenyl POSS as the initiator. The novel organic−inorganic amphiphile was incorporated into epoxy resin to prepare the organic−inorganic hybrid thermosets. The morphology of the organic−inorganic hybrids was characterized by means of atomic force microscopy (AFM) and transmission electron microscopy (TEM). It is found that the epoxy thermosets displayed a variety of nanostructures depending on the concentration of the POSS-capped PCL. The formation of nanostructures was addressed on the basis of miscibility and phase behavior of the subcomponents (viz. POSS and PCL chains) of the organic−inorganic amphiphile with epoxy after and before curing reaction. It is judged that the nanostructures in the organic−inorganic hybrid composites were formed via a mechanism of self-assembly. The static contact angle measurements show that the organic−inorganic nanocomposites displayed a significant enhancement in surface hydrophobicity as well as reduction in surface free energy. The improvement in surface properties was ascribed to the enrichment of POSS moiety on the surface of the nanostructured thermosets, which was evidenced by X-ray photoelectron spectroscopy.

Introduction

The morphological control of thermosets at the nanometer level is long a pursuit in the studies of polymer materials;[1] the formation of nanostructures in thermosets can further optimize the properties of materials. The preparation of nanostructured thermosets can generally be categorized into two approaches: (i) self-assembly[2,3] and (ii) reaction-induced microphase separation.[4] The first route is a templating technique where the mixture composed of amphiphilic and reactive compounds is self-assembled to form various micelle structures. The morphology at the nanometer can be fixed via the cross-linking of reactive components. Bates et al.[2] proposed the strategy of creating the nanostructures in thermosets using amphiphilic block copolymers. In the protocol, precursors of thermosets act as selective solvents of block copolymers, and some self-assembled morphologies such as spherical, lamellar, hexagonally packed cylindrical, or cubic structures are formed depending on the compositions of the blends before curing reaction. The micelle structures can further be fixed with adding hardeners and subsequent curing. During the past years, a variety of block copolymer architectures have been used to obtain some equilibrium ordered (or disordered) nanostructures thermosets.[3] The role of curing reaction is to lock in the morphology that is already present although it was identified that there are some small changes in the nanostructures after and before curing reaction.[2] More recently, it is proposed that the nanostructured thermosets can alternatively be prepared via the approach of reaction-induced microphase separation; i.e., the nanostructures can be accessed by controlling the microphase separation of a part of subchains of amphiphilic block copolymers induced by polymerization whereas the other subchains still remain miscible with the cross-linked thermosets.[4]

It is crucial to prepare the amphiphilic compounds for the control of the formation of nanostructures. During the past years, a great number of amphiphilic organic block copolymers were synthesized for preparing nanostructured thermosets. Nonetheless, the utilization of organic−inorganic amphiphilic compounds for nanostructured thermosets remains largely unexplored. Organic−inorganic hybrid composites have attracted considerable interest since this class of materials can combine the advantages of inorganic materials with those of organic polymers. Generally, inorganic compounds are immiscible with organic polymers due to the big difference in solubility parameters.[5] It is ideal to combine the features of miscibility to fulfill organic and inorganic amphiphilicity. Polyhedral oligomeric silsesquioxanes (POSS) are a class of important nanosized cagelike molecules (Scheme 1) derived from hydrolysis and condensation of trifunctional organosilanes. POSS molecules possess a formula of $[RSiO_{3/2}]_n$, n is an even number in the range of 6−12, where R can be various types of organic groups, one (or more) of which is reactive or polymerizable. Polymers incorporated with the well-defined nanosized POSS cages represent a class of important organic−inorganic nanocomposites.[6] During the past decade, the ample literature on the organic−inorganic thermosetting nanocomposites containing POSS has appeared.[7] Lee and Lichtenhan[7a] reported that the molecular level reinforcement provided by the POSS cages could significantly retard the physical aging process of epoxy thermosets in the glassy state. Laine et al.[7b−g] investigated the modifications of epoxy by a series of octasilsesquioxanes with a variety of R groups such as aminophenyl and dimethylsiloxypropylglycidyl ether groups and found that the dynamic mechanical properties, fracture toughness, and thermal stability of the epoxy hybrids were closely dependent on the types of R groups, tether structures between epoxy matrices and POSS cages, the defects in silsesquioxane cages, etc. Williams et al.[7h] observed that a primary liquid−liquid phase separation occurred at the time of adding the POSS-diamine precursors to epoxy due to the incompatibility between epoxy and isobutyl POSS glycidyl. It is noted that the nature of the organic inert groups and prereaction of a monofunctional POSS have a pronounced

* To whom all correspondence should be addressed: e-mail szheng@sjtu.edu.cn; Tel +86-21-54743278; Fax +86-21-54741297.

10.1021/ma0709351 CCC: $37.00
Published on Web 08/28/2007

Scheme 1. Synthesis of Polyhedral Oligomeric Silsesquioxane (POSS)-Capped PCL

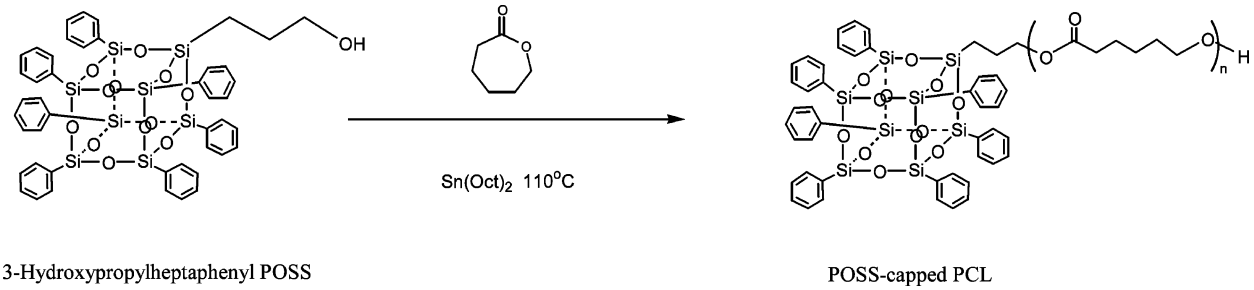

3-Hydroxypropylheptaphenyl POSS

POSS-capped PCL

impact on the morphology of the resulting POSS-modified polymer networks.[7i] Zheng et al.[7j] reported that the different morphological structures could be formed in the POSS-containing hybrid composites depending on the types of R groups; moreover, the phase-separated composites and nanocomposites could be prepared by adjusting the degrees of reaction between epoxy matrix and POSS macromer. Matejka et al.[7k,l] investigated the structure and properties of epoxy networks reinforced with POSS, and the effects of POSS−POSS interactions on the thermal properties were addressed. All the previous studies reported the modification of epoxy thermosets using a variety of functional POSS macromers. To the best of our knowledge, the control of nanostructures in thermosets using a POSS-capped macromolecular amphiphile has not been reported yet.

In the present work, we designed and synthesized POSS-capped poly(ϵ-caprolactone) (PCL). The POSS-capped PCL is a novel amphiphilic macromolecule due to the presence of organic (viz. PCL chain) and inorganic (viz. silsesquioxane cage) portions. The organic−inorganic amphiphile was incorporated into epoxy resin to prepare the nanostructured thermosets. It is expected that the formation of the nanostructures follows the mechanism of self-assembly since it has been known that (i) PCL subchain is miscible with epoxy after and before the curing reaction[8] and (ii) octaphenyl POSS is immiscible with epoxy resin after and before curing reaction. Atomic force microscopy (AFM), transmission electron microscopy (TEM), and differential scanning calorimetry (DSC) were used to investigate the morphology of the thermosets, and the formation mechanism of the nanostructures is addressed by investigating the miscibility and phase behavior of the systems after and before curing reaction. The surface properties of the nanostructured thermosets were addressed on the basis of static contact angle measurements and X-ray photoelectron spectroscopy (XPS).

Experimental Section

Materials. Epoxy monomer used in this work is diglycidyl ether of bisphenol A (DGEBA) which was obtained from Shanghai Resin Co., China, and its epoxide equivalent weight was measured to be 177. 4,4′-Methylenebis(2-chloroaniline) (MOCA) is of chemically pure grade and was used as the curing agent, purchased from Shanghai Reagent Co., China. Octaphenyl polyhedral oligomeric silsesquioxane (POSS) was prepared via hydrolysis and rearrangement of phenyltrimethoxylsilane.[9a] The monomer, ϵ-caprolactone (CL), was purchased from Fluka Co. Germany, and it was distilled over CaH_2 under decreased pressure prior to use. Stannous(II) octanoate [$Sn(Oct)_2$] is of analytically pure grade and was purchased from Shanghai Reagent Co., China. The solvents such as tetrahydrofuran (THF), dichloromethane (CH_2Cl_2), ethanol, and petroleum ether (distillation range: 60−90 °C) were obtained from Shanghai Reagent Co., Shanghai, China. Before use, tetrahydrofuran (THF) was refluxed over sodium, distilled, and then stored in a sealed vessel with the molecular sieve of 4 Å.

3-Hydroxypropylheptaphenyl polyhedral oligomeric silsesquioxane (POSS) was used as the initiator for the ring-opening polymerization of ϵ-caprolactone (CL) to prepare the POSS-capped PCL, the preparation of which was detailed in the previous work.[9b] The ring-opening polymerization (ROP) of ϵ-caprolactone (CL) catalyzed by stannous(II) octanoate [$Sn(Oct)_2$] was employed to prepare POSS-capped poly(ϵ-caprolactone) (PCL) using 3-hydroxypropylheptaphenyl POSS as the initiator, as illustrated in Scheme 1. The synthesis and characterization of POSS-capped PCL have been depicted in the previous work. In this work, the molecular weight of the organic−inorganic amphiphile was controlled to be $M_{n,NMR} = 2490$ to ensure the volume ratio of the inorganic moiety (viz. silsesquioxane) to organic part (i.e., PCL chain) to be ca. 1:1.

Synthesis of Model Poly(ϵ-caprolactone). The model PCL with the molecular weight identical with the chain length of PCL in the POSS-capped PCL was synthesized via the ring-opening polymerization (ROP) of ϵ-CL with benzyl alcohol as the initiator. Typically, benzyl alcohol (1.08 g, 10 mmol) and ϵ-CL (13.92 g, 122.11 mmol) were charged to a 100 mL round-bottom flask equipped with a dry magnetic stirring bar, and $Sn(Oct)_2$ (1/1000 wt with respect to ϵ-CL) was added. The flask was connected to a standard Schlenk line, and the reactive mixture was degassed via three pump freeze−thaw cycles and then immersed in a thermostated oil bath at 120 °C for 24 h. The crude product was dissolved in tetrahydrofuran, and the solution was dropped into an excessive amount of petroleum ether to afford the precipitates, and this procedure was repeated three times to obtain white solids. The product was dried in a vacuum oven until a constant weight was accessed with a yield of 96%. The molecular weight was determined by means of ^{1}H NMR spectroscopy and was calculated according to the ratio of integration intensity of aliphatic methylene protons to aromatic protons to be $M_n = 1620$.

Preparation of Nanostructured Epoxy Resin. The POSS-capped PCL with $M_{n,NMR} = 2490$ was added to DGEBA at ambient temperature with continuous stirring until the system became homogeneous and transparent. Then the curing agent, MOCA, was added to system with vigorous stirring until the curing agent was fully dissolved. The ternary mixture was poured into Teflon molds and cured at 80 °C for 2 h, 160 °C for 2 h, and 180 °C for 2 h to access a complete curing reaction. The thermosetting blends containing POSS-capped PCL up to 40 wt % were obtained.

Measurement and Techniques. *Nuclear Magnetic Resonance Spectroscopy (NMR).* The ^{1}H NMR and ^{13}C NMR measurements were carried out on a Varian Mercury Plus 400 MHz NMR spectrometer at 25 °C. The samples were dissolved with deuterated $CDCl_3$, and the solutions were measured with tetramethylsilane (TMS) as an internal reference. The high-resolution solid-state ^{29}Si NMR spectra were obtained using cross-polarization (CP)/magic angle spinning (MAS) together with the high-power dipolar decoupling (DD) technique. The 90° pulse width of 4.1 μs was employed with free induction decay (FID) signal accumulation, and the cross-polarization (CP) Hartmann−Hahn contact time was set at 3.5 ms for all the measurements. The rate of MAS was 4.0 kHz for measuring the spectra. The Hartmann−Hahn CP matching and dipolar decoupling field was 57 kHz. The chemical shifts of all ^{29}Si spectra were determined by taking the silicon of solid Q_8M_8 relative to TMS as an external reference standard.

Fourier Transform Infrared Spectroscopy (FTIR). The FTIR measurements were conducted on a Perkin-Elmer Paragon 1000 Fourier transform spectrometer at room temperature (25 °C). The

sample films were prepared by dissolving the POSS-capped PCL with $CHCl_3$ (5 wt %), and the solutions were cast onto KBr windows. The residual solvent was removed in a vacuum oven at 60 °C for 2 h. The samples of thermosets were mixed with the powder of KBr and then pressed into the small flakes. All the specimens were sufficiently thin to be within a range where the Beer−Lambert law is obeyed. In all cases 64 scans at a resolution of 2 cm^{-1} were used to record the spectra.

Differential Scanning Calorimetry (DSC). Differential scanning calorimetry (DSC) was carried out with a Perkin-Elmer Pyris 1 differential scanning calorimeter in a dry nitrogen atmosphere. An indium standard was used for temperature and enthalpy calibrations. All of the samples (about 10 mg in weight) were first heated to 180 °C and held at this temperature for 3 min to remove the thermal history, followed by quenching to −50 °C. A heating rate of 20 °C/min was used at all cases. The glass transition temperature (T_g) was taken as the midpoint of the heat capacity change. The crystallization temperatures (T_c) and the melting temperatures (T_m) were taken as the temperatures of the minimum and the maximum of both exothermic and endothermic peaks, respectively.

Transmission Electron Microscopy (TEM). Transmission electron microscopy (TEM) was performed on a JEOL JEM-2010 transmission electron microscope at an acceleration voltage of 120 kV. The samples were trimmed using an ultrathin microtome machine, and the section samples (ca. 70 nm in thickness) were placed in 200 mesh copper grids for observations.

Atomic Force Microscopy (AFM). The thermosets samples were trimmed using a an ultrathin microtome machine, and the specimen sections (ca. 70 nm in thickness) were used for AFM observations. The AFM experiments were performed with a Nanoscope IIIa scanning probe microscope (Digital Instruments, Santa Barbara, CA). Tapping mode was employed in air using a tip fabricated from silicon (125 μm in length with ca. 500 kHz resonant frequency). Typical scan speeds during recording were 0.3∼1 lines s^{-1} using scan heads with a maximum range of 16 μm × 16 μm.

Contact Angle Measurements. In order to prepare the specimens for contact angle measurement, all the components were dissolved with a smallest amount of THF. The mixtures composed of DGEBA, MOCA, and POSS-capped PCL were cast on glass sliders, and the thickness of films was controlled to about 20 μm. The solvent was slowly evaporated at room temperature, and the residual solvent was eliminated in vacuo for 48 h before the samples were cured at 80 °C for 2 h, 160 °C for 2 h, and 180 °C for 2 h. The flat free surfaces of the thermosets were used for the measurement of contact angle. The static contact angle measurements with ultrapure water and ethylene glycol were carried out on a KH-01-2 contact angle measurement instrument (Beijing Kangsente Scientific Instruments Co., China) at room temperature. The samples were dried at 60 °C in the vacuum oven for 24 h prior to measurement.

X-ray Photoelectron Spectroscopy (XPS). The XPS was measured with VG ESCALAB MK II at room temperature by using an Mg KR X-ray source (h_ν = 1253.6 eV) at 14 kV and 20 mA. The sample analysis chamber of the XPS instrument was maintained at a pressure of 1×10^{-7} Pa. To determine the composition on the top layer of the film, the tilting angle is 5°. The binding energies were calibrated by using the containment carbon (C 1s = 284.6 eV). A linear background method removed the XPS background, and the peaks analysis was carried out by using the curve-fitting software.

Results and Discussion

Preparation of POSS-Capped PCL and Thermosets. The synthetic route of the organic−inorganic amphiphile, POSS-capped PCL, is shown in Scheme 1. 3-Hydroxypropylheptaphenyl POSS [$(HOCH_2CH_2CH_2)(C_6H_5)_7Si_8O_{12}$][9b] was used as the initiator, and the ring-opening polymerization of ϵ-caprolactone was catalyzed by stannous(II) octanoate [$Sn(Oct)_2$] and was carried out at 110 °C for 24 h. By controlling the molar ratios of 3-hydroxypropylheptaphenyl POSS to ϵ-caprolactone (CL), the POSS-capped PCL with various molecular weights can be obtained.[9c] In this work, the molecular weight of the organic−inorganic amphiphile was controlled to be $M_{n,NMR}$ = 2490 to ensure the volume ratio of the inorganic moiety (viz. silsesquioxane) to organic part (i.e., PCL chain) to be ca. 1:1.

The POSS-capped PCL amphiphile was incorporated into the precursors of epoxy resin (viz. DGEBA and MOCA), and the mixtures were cured at elevated temperature. Before curing, all the ternary mixtures composed of DGEBA, POSS-capped PCL, and MOCA were homogeneous and transparent, suggesting that no macroscopic phase separation occurred at room and curing temperatures. After cured at the elevated temperatures, the thermosets were obtained with the POSS-capped PCL contents up to 40 wt %. It is noted that all the cured products investigated are homogeneous and transparent, suggesting that no macroscopic phase separation occurred at the scale exceeding the wavelength of visible light as the curing reaction proceeded. The morphologies of the thermosets were investigated by atomic force microscopy (AFM) and transmission electronic microscopy (TEM).

Nanostructures in Epoxy Thermosets. Shown in Figure 1 are the AFM images of the thermosets containing 10, 20, 30, and 40 wt % of the POSS-capped PCL. The left and right are the topography and phase images, respectively. The topography images showed that the surfaces of the as-prepared specimens are free of visible defects, and thus the effect of roughness resulting from the specimen preparation on morphology can be negligible. It is noted that all the thermosetting blends exhibited nanostructured morphologies. In terms of the volume fraction of POSS moiety and the difference in viscoelastic properties between the organic and inorganic portions, the light continuous regions are attributed to the cross-linked epoxy matrix, which could be interpenetrated by the PCL chains of POSS-capped PCL, while the dark regions are assignable to POSS domains. In the thermoset containing 10 wt % of POSS-capped PCL case, the nanosized particles were homogeneously dispersed in the continuous epoxy matrix with the average size of ca. 10 nm in diameter, as shown in Figure 1A. With the increase of the content of POSS-capped PCL, the separate POSS nanodomains began to aggregate in the continuous epoxy network, and some interconnected objects of POSS nanodomains appeared (Figure 1B). When the concentration of POSS-capped PCL was more than 30 wt %, the POSS nanodomains were almost self-organized into the interconnected nanoobjects, as shown in Figure 1C,D. The nanostructures can be further confirmed by means of transmission electronic microscopy (TEM).

Figure 2 shows the TEM micrographs of the thermosets containing the POSS-capped PCL amphiphile. It is noted that the heterogeneous morphology at the nanometer scale was found in all the cases. Because of the difference in transmitted electronic density between organic and inorganic portion (viz. POSS moiety), the dark area are assignable to the POSS portion, which is covalently connected with PCL chain. For the thermoset containing 10 wt % POSS-capped PCL, it is seen that the spherical POSS domains were dispersed in the continuous epoxy matrix with the average size of ca. 5.0 nm, as shown in Figure 2A. With increasing the concentration of POSS-capped PCL, it is seen that distance between the adjacent POSS nanodomains decreased while the size of the nanodomains remained almost invariant. In addition, it is noted that with increasing the content of POSS-capped PCL the nanodomains gradually became interconnected nanoobjects (see Figure 2B,C). Shown in Figure 2D is the TEM micrograph of the thermoset containing 40 wt % POSS-capped PCL. It is seen that the POSS nanodomains were highly interconnected, and a bicontinuous

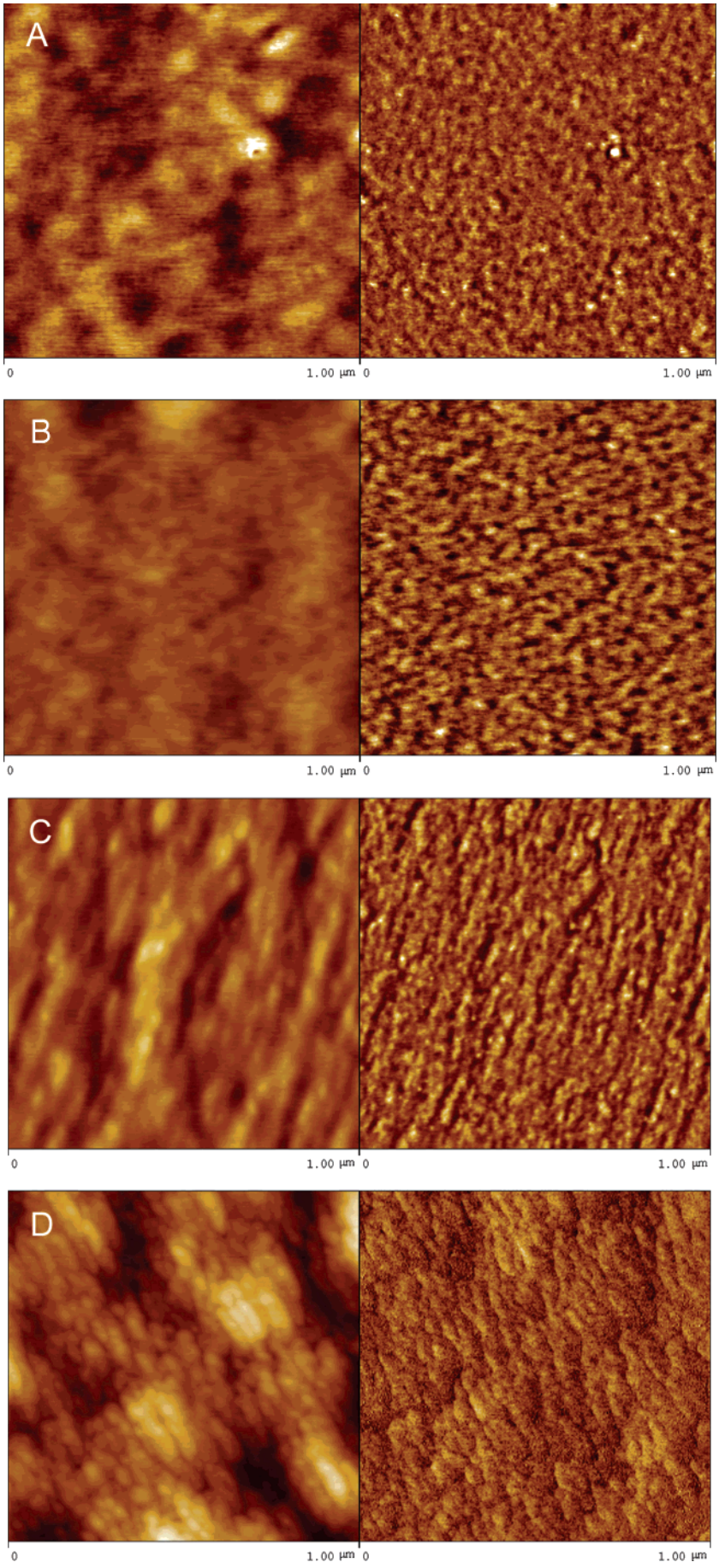

Figure 1. AFM images of the thermosets containing (A) 10, (B) 20, (C) 30, and (D) 40 wt % of POSS-capped PCL. Left: topography; right: phase contrast.

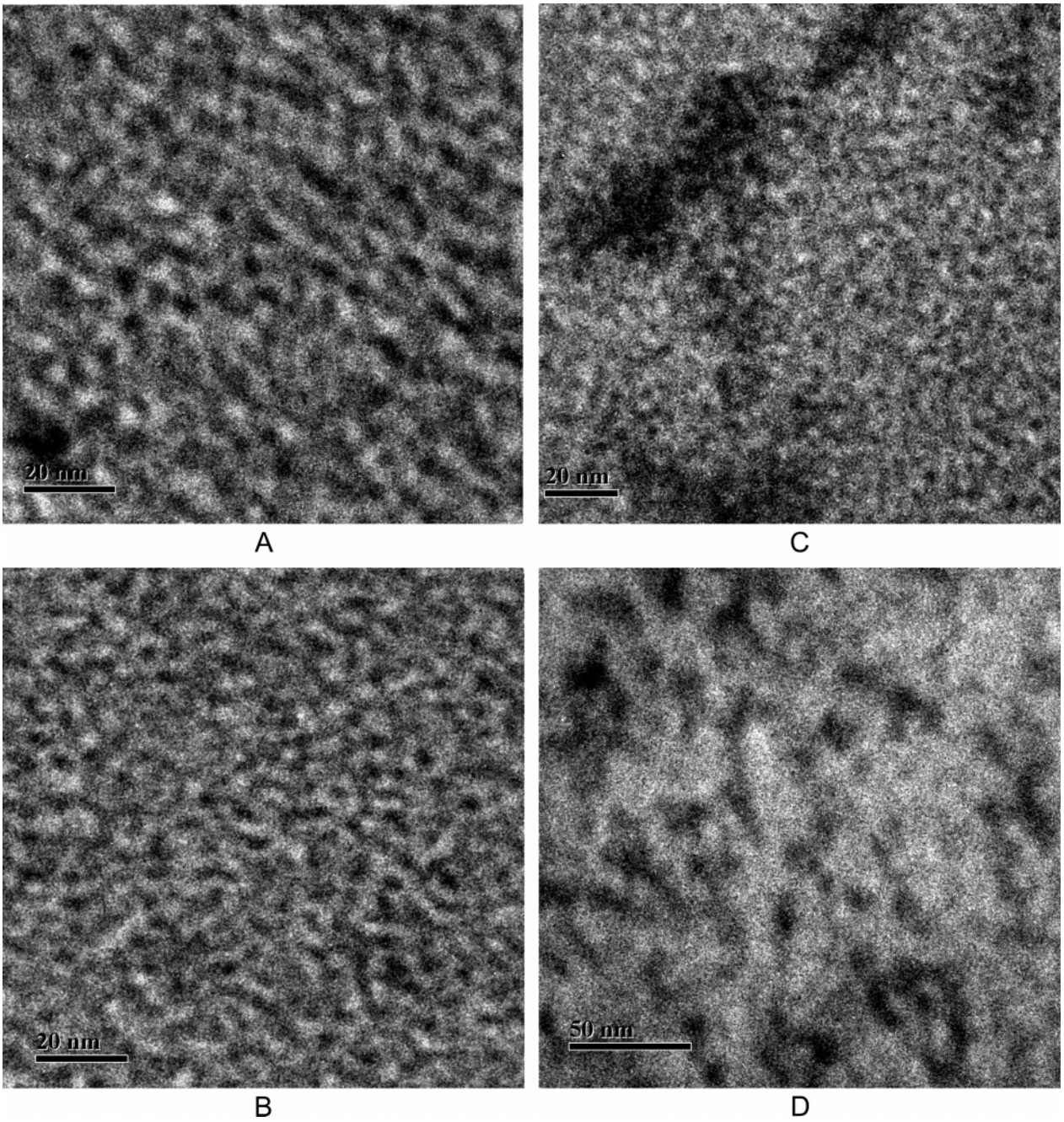

Figure 2. TEM images of the thermosets containing (A) 10, (B) 20, (C) 30, and (D) 40 wt % of POSS-capped PCL.

microphase-separated morphology was exhibited. It should be pointed out that there is a little difference between the micrographs of TEM and AFM since the two techniques detect the information on morphology of the thermosets from different side views of structure. The TEM micrographs are obtained on the basis of the difference in transmitted electronic densities through samples whereas the AFM micrographs reflect the information about tip−sample interactions resulting from adhesion,[10a] surface stiffness,[10b] and viscoelastic effects.[10c−e] Therefore, the AFM results could be more sensitive to the transition region between POSS nanodomains and epoxy matrices that were interpenetrated by PCL chains. The AFM and TEM results indeed indicated that the nanostructured epoxy thermosets were obtained.

It is of interest to examine the behavior of crystallization of the organic−inorganic hybrid nanocomposites since the sub-blocks of the POSS-capped PCL (i.e., POSS and PCL) are crystalline. Shown in Figure 3 are the profiles of wide-angle X-ray diffraction for octaphenyl POSS, the POSS-capped PCL, and the hybrid nanocomposites. For octaphenyl POSS, the appearance of sharp diffraction peaks indicates that the POSS is highly crystalline.[9a,d] In the curve of POSS-capped PCL, the intense diffraction peaks located at $2\theta = 21.39°$, 22.00°, 23.70°, and 43.99° was assigned to the (110), (111), and (200) reflections of PCL.[11] In addition, a new diffraction peak was seen at $2\theta = 7.28°$. The new diffraction peak could be related to the aggregation of POSS blocks. Because of the immiscibility between PCL chains and POSS portion, the terminal POSS blocks could be self-assembled into microdomains, which could display the similar diffraction profile as octaphenyl POSS.[9a] For the nanostructured thermosets, all the XRD diffraction curves displayed a broad amorphous halo at ca. $2\theta = 18^{o}$, and no diffraction peaks assignable to PCL subchain were detected. This observation indicates that the PCL subchain is no longer

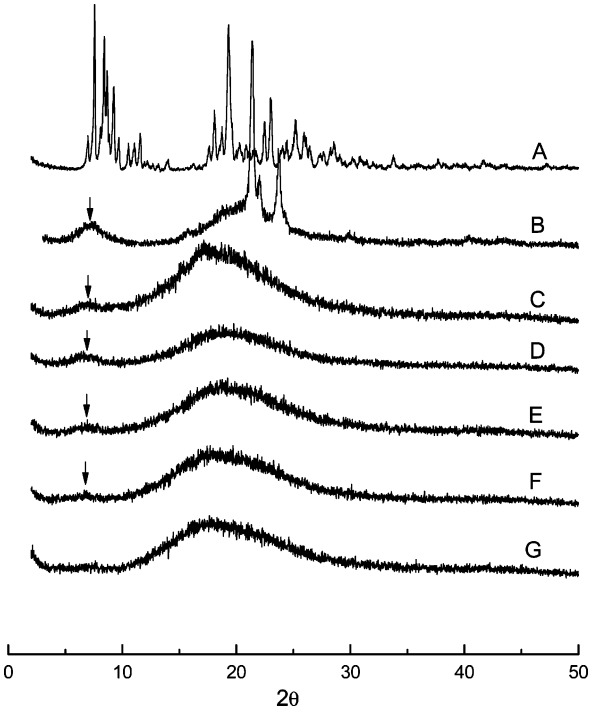

Figure 3. Profile of wide X-ray diffraction: (A) octaphenyl POSS; (B) POSS-capped PCL; (C) thermosets containing 40 wt %; (D) thermosets containing 30 wt %; (E) thermosets containing 20 wt %; (F) thermosets containing 10 wt %; (G) control epoxy.

crystallizable in the nanocomposites. In addition to the amorphous halo at ca. $2\theta = 18^{o}$, a small diffraction maximum at $2\theta = 7.28°$ was observed for all the POSS-capped PCL-containing thermosets. The intensity of the peaks increased with increasing the concentration of POSS-capped PCL. It is plausible to propose that the diffraction peaks are attributed to the aggregation of POSS blocks in the thermosets. The similar observation was previously found in other monofunctionalized POSS-containing epoxy thermosets.[7h,j-l] This result further substantiates the presence of POSS microdomains in the thermosets, which is in a good agreement with those obtained by means of TEM and AMF.

Formation Mechanism of Nanostructures. It is crucial for the determination of the formation mechanism of the nanostructures in the thermosetting system to know the miscibility and phase behavior of the subcomponents (viz. POSS and PCL chains) of the organic−inorganic amphiphilic macromolecule with epoxy resin after and before curing reaction. In order to examine the miscibility of epoxy resin with POSS, octaphenyl POSS was selected as the model compound for the POSS terminal group of the organic−inorganic amphiphile. It was observed that at room and elevated temperature (e.g., 150 °C) all the mixtures were heterogeneous and cloudy, and macroscopic phase separation was seen. This observation indicates that the POSS is immiscible (or insoluble) with the precursors of epoxy resin. In contrast, all the mixtures of epoxy resin with the model PCL are transparent and homogeneous at 80 °C (above the melting point of PCL) and 150 °C (i.e., the curing temperature), implying that no phase separation occurred at the scale exceeding the wavelength of visible lights. The single, composition-dependent glass transition temperatures (T_g's) of the blends indicate that the aromatic amine-cured epoxy was fully miscible with the PCL after and before curing. This result is consistent with the conclusions based on the thermosetting blends of epoxy resin with the PCL of high molecular weights.[8] It was proposed that before curing reaction the miscibility is ascribed to the non-negligible contribution of mixing entropy (ΔS_m) to free energy of mixing (ΔG_m) since the molecular weights of epoxy precursors are quite low. After the curing reaction, the miscibility was attributed to the formation of the intermolecular hydrogen-bonding interactions between the aromatic amine-cross-linked epoxy and PCL.[8] The difference in miscibility of the subconstituents of the organic−inorganic amphiphile implies that the formation of nanostructures in the present thermosetting system followed a mechanism of self-assembly. It is plausible to propose that in the mixtures of the precursors of epoxy resin with POSS-capped PCL the precursors of epoxy (viz. DGEBA and MOCA) act as the selective solvent of the organic−inorganic amphiphile, and thus the self-organized nanostructures will be formed. Depending on the volume fraction of the POSS-capped PCL in the mixtures, various nano-objects could be obtained. The nanostructures would be further locked in via the curing reaction at elevated temperature, as depicted in Scheme 2.

The organic−inorganic nanostructured thermosets were subjected to thermal analysis, and the DSC curves are shown in Figure 4. In the DSC thermogram of POSS-capped PCL a sharp endothermic peak at 47.7 °C was displayed, which is assignable to the melting transition of PCL chain of the organic−inorganic amphiphile. It is noted that all the thermosets investigated did not exhibit the melting transition of PCL subchains, suggesting that the PCL subchains are not crystalline in the nanostructured thermosets. It is plausible to propose that the PCL subchains are miscible with the epoxy thermosets and could interpenetrate with the cross-linked epoxy networks. The miscibility was further evidenced by the depression in glass transition temperatures (T_g's) for the epoxy-rich phases, as shown in Figure 4. It is seen that each thermoset containing POSS-capped PCL displayed single T_g, which decreased with increasing the concentration of POSS-capped PCL. The decreased T_g's resulted from the plasticization of miscible PCL on epoxy matrix. There are several theoretical and empirical equations to describe the dependence of glass transition temperature on blend composition.[12] Of them, the Couchman equation[12c] is frequently used:

$$\ln T_g = [W_1 k \ln T_{g1} + W_2 \ln T_{g2}]/(W_1 k + W_2) \qquad (1)$$

where W_i is the weight fraction of component i and T_g is the glass transition temperature of blend. The parameter k is Couchman coefficient defined by

$$k = \Delta C_{p1}/\Delta C_{p2} \qquad (2)$$

where ΔC_{pi} designates the increment of the heat capacity of the specimen at glass transition. In the present work, the value of k for the miscible epoxy blends with the model PCL with the molecular weights identical with the chain length of PCL in the organic−inorganic amphiphile was determined to be 1.71, as shown in Figure 5. However, it is noted that the T_g's of the nanostructured thermosets containing POSS-capped PCL are significantly higher than those of the binary thermosetting blends of epoxy and PCL at the same compositions of epoxy and PCL (Figure 5). It is proposed that the increased T_g's for the nanocomposites could be associated with the formation of the nanostructures in the composites. In the binary thermosetting blends of epoxy resin with PCL, the PCL chains can be homogeneously dispersed into the epoxy matrix and were well interpenetrated into the cross-linked epoxy networks via the formation of the intermolecular hydrogen-bonding interactions. In contrast, the PCL chains have to be enriched at the surface of the microphase-separated POSS nanodomains due to the

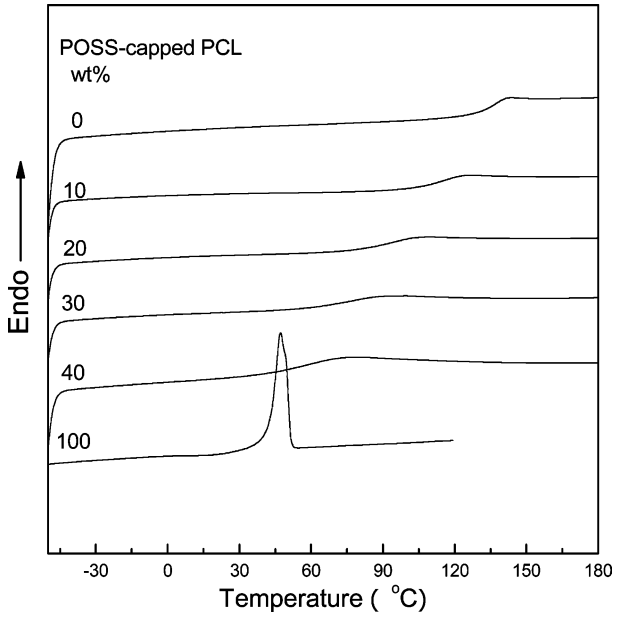

Figure 4. DSC curves of the nanostructured epoxy thermosets.

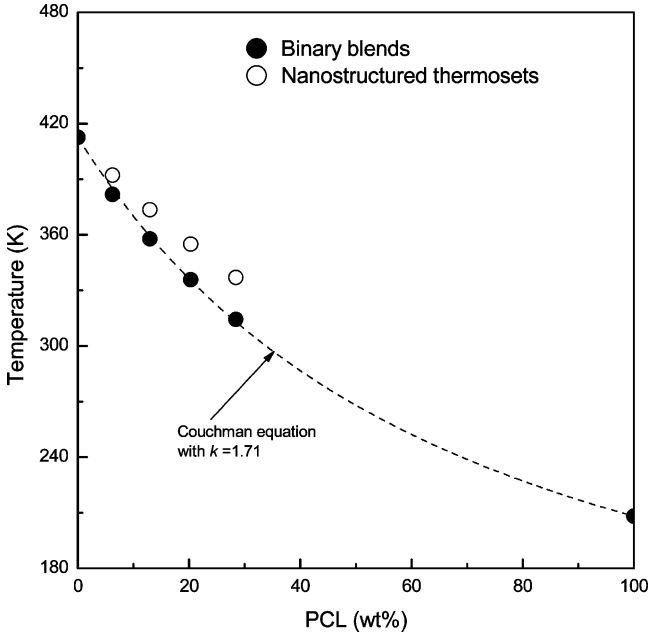

Figure 5. Plots of glass transition temperature as functions of PCL contents for the nanostructured thermosets. For the sake of comparison, the variation of T_g's of the binary thermosetting blends of epoxy with the model PCL is also incorporated into this figure.

presence of chemical bonds between POSS terminal groups and PCL chains in the composites. Because of the steric hindrance, the PCL chains at the intimate surface of POSS nanodomains could not be well mixed with epoxy matrix. Compared to the binary blends of epoxy with PCL, there are less PCL chains that are mixed with epoxy matrix in the nanocomposites; i.e., the plasticization of PCL chains on the epoxy matrix would be effectively weakened, and thus the higher T_g's of epoxy matrix were exhibited. This effect has been reported in the self-assembly of epoxy resin and amphiphilic block copolymer nanocomposites.[2] Using the value of k coefficient for the blend of epoxy and the model PCL, the fraction of the demixed (or deswelled) PCL can be estimated according to the Couchman equation. The results are summarized in Table 1. It is noted that the fraction of demixed (or deswelled) PCL is 2−10 wt % in the nanostructured thermosets containing 10−40 wt % POSS-capped PCL.

The miscibility of the PCL chains of the organic−inorganic amphiphile with the cross-linked epoxy resin is ascribed to the formation of the intermolecular hydrogen-bonding interactions, which is readily evidenced by Fourier transform infrared spectroscopy (FTIR). The FTIR spectra of POSS-capped PCL and the nanostructured thermosets in the range of 1660−1800 cm^{-1} are shown in Figure 6. The absorption bands are ascribed to the stretching vibration of carbonyl groups (〉C═O)

Scheme 2. Preparation of Nanostructured Epoxy Thermosets

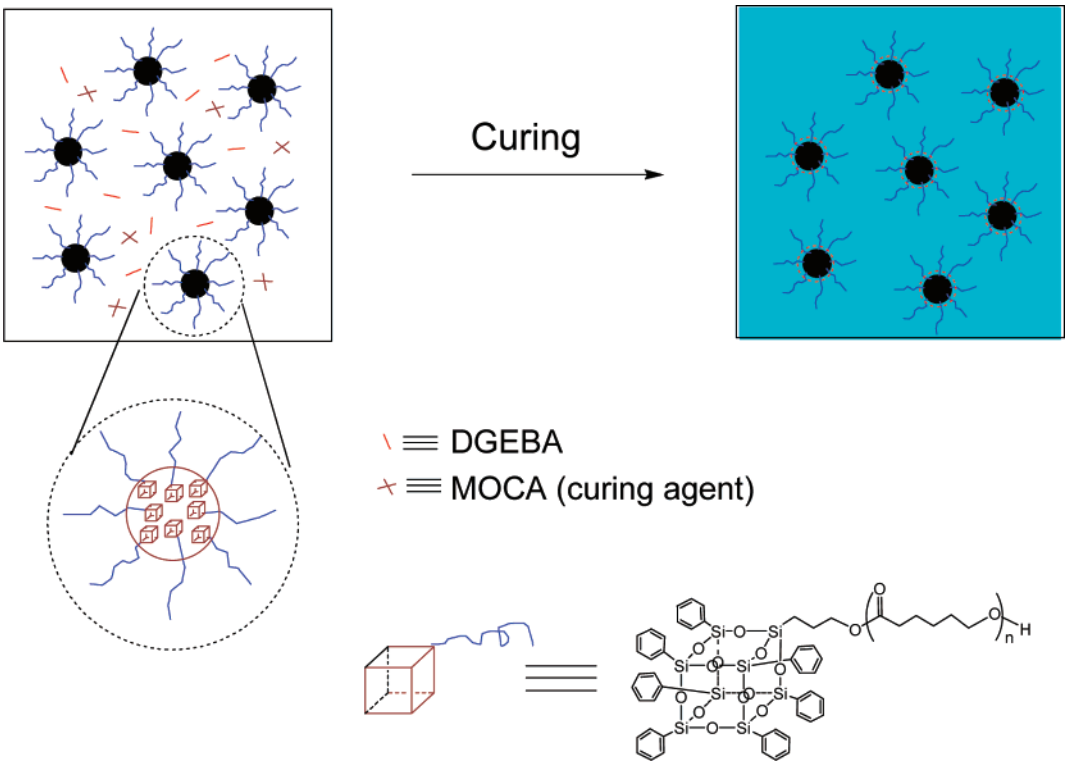

Table 1. Analysis of Demixed PCL in the Nanostructured Epoxy Thermosets Containing POSS-Capped PCL

POSS-capped PCL (wt %)	PCL fraction (wt %)[a]	T_g (°C)[b]	demixed PCL (wt %)[c]
0		139.4	
10	6.19	119.0	1.72
20	12.93	100.5	3.93
30	20.29	81.9	6.17
40	28.37	63.8	8.63
100	66.70	−65.0	

[a] PCL fraction is calculated by deducting the percentage of POSS portion. [b] Experimental T_g's of the nanostructured thermosets. [c] The demixed PCL fraction is estimated according to Couchman equation with $k = 1.71$, which was determined from the binary thermosetting blends of epoxy and the model PCL.

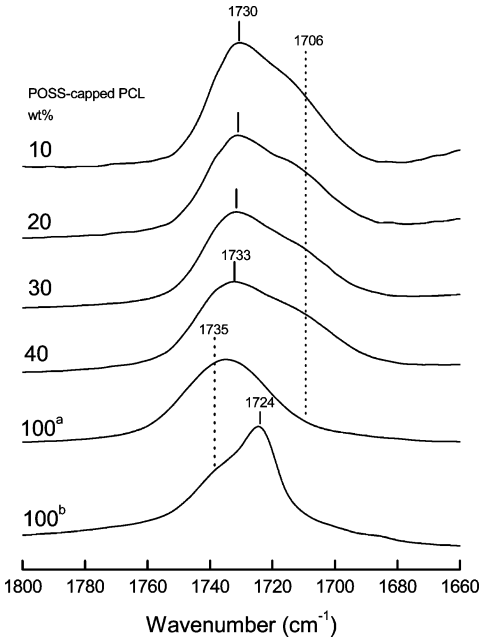

Figure 6. FTIR spectra of the nanostructured thermosets in the range of 1660−1800 cm^{-1}: (a) at 80 °C; (b) at 25 °C.

of PCL chains. At the room temperature, the carbonyl band of the POSS-capped PCL consists of two components sensitive to the conformation of PCL chains. The one component centered at 1735 cm^{-1} is characteristic of amorphous chains of PCL whereas the sharp band at 1724 cm^{-1} is ascribed to the carbonyls in the crystalline region of PCL. Upon heating the organic−inorganic amphiphile up to 80 °C, the band at 1724 cm^{-1} disappeared owing to the fusion of PCL crystals. It is noted that in the FTIR spectra of the nanostructured thermosets the bands of PCL crystals at 1724 cm^{-1} were absent, implying that the PCL chains exist in the thermosets in the amorphous state. Nonetheless, there appeared new shoulders at the lower frequency of 1706 cm^{-1} in the FTIR spectra of the nanostructured thermosets, and the shoulder bands are assigned to the stretching vibration of hydrogen-bonded carbonyls;[13] i.e., there is the formation of the intermolecular hydrogen-bonding interactions between the secondary hydroxyl groups of epoxy matrix and the carbonyl groups of PCL. In addition, the bands at 1735 cm^{-1} were found to shift to the lower frequency (1730 cm^{-1}) with increasing the concentration of POSS-capped PCL. The FTIR results indicate that there existed the intermolecular hydrogen-bonding interactions between the PCL chains of the POSS-capped PCL and the epoxy networks.

It is possible to resolve the nonassociated and the associated carbonyl bands using the spectral curve-fitting method. The Gaussian line shape function was used in this fitting procedure,

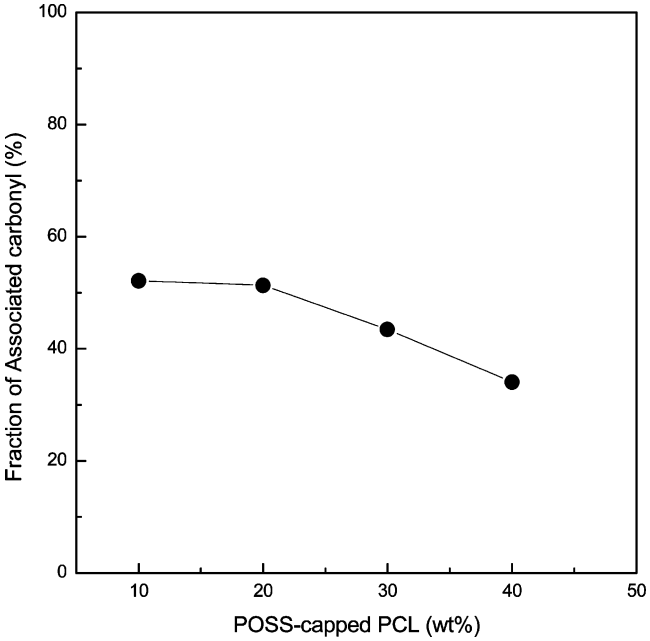

Figure 7. Variation of fraction of associated carbonyls as a function of POSS-capped PCL in the nanostructured thermosets.

and the good fitting was carried out. The F^f_{CO} is the fraction of the nonassociated carbonyl bands, calculated from the values of absorbency for the associated and the nonassociated band contributions:

$$F^f = \frac{A_f}{A_f + \left(\frac{\epsilon_f}{\epsilon_a}\right)A_a} \times 100\% \quad (3)$$

where ϵ_i is the molar absorption coefficient. The subscripts f and a stand for free and associated carbonyl groups, respectively. To carry out this calculation, we require the knowledge of the molar absorption coefficients (ϵ_f and ϵ_a) or their ratio (ϵ_f/ϵ_a) for the nonassociated and associated carbonyl bands. Using the ϵ_f/ϵ_a value of 1.3 for the interassociation of ester type carbonyls with the hydroxyls of poly(hydroxyether of bisphenol A) blends determined by Coleman et al.,[13] we calculated the fraction of nonassociated carbonyl bands. The variation of F^f_{CO} as a function of temperature is shown in Figure 7. It is seen that the fractions of associated carbonyls decreased with increasing the concentration of POSS-capped PCL.

Surface Properties of Nanostructured Thermosets. It is known that organosilicon compounds are generally of low surface energy. In the present case, the organosilicon moiety (viz. silsesquioxane cage) was covalently connected with PCL chains. It is plausible to propose that when the POSS-capped PCL was incorporated into organic polymers, the inorganic portion could be enriched at the surface of materials, and thus the surface hydrophobilicity of the nanocomposites will be improved. In this work, the surface properties of the organic−inorganic nanocomposites were investigated in terms of the measurement of static contact angle. The contact angles were measured with water and glycol as probe liquids, and the results are summarized in Table 2. The contact angle of the control epoxy was estimated with water to be ca. 85.2°. Upon adding POSS-capped PCL to the system, the contact angles are increased, and the water contact angle for the organic−inorganic nanocomposites containing 40 wt % POSS-capped PCL was increased up to 96.2°. This observation indicates that the

Table 2. Static Contact Angles and Surface Free Energy of Epoxy Thermosets Containing POSS-Capped PCL[a]

POSS-capped PCL (wt %)	θ_{H_2O} (deg)	$\theta_{\text{ethylene glycol}}$ (deg)	γ_s^d (mN m^{-1})	γ_s^p (mN m^{-1})	γ_s (mN m^{-1})
0	85.2 ± 0.7	57.8 ± 1.0	25.50	4.94	30.44
10	92.9 ± 0.9	69.3 ± 0.9	20.46	3.54	24.00
20	95.9 ± 0.5	74.9 ± 0.8	16.81	3.58	20.39
30	100.5 ± 0.8	78.1 ± 1.1	18.29	1.88	20.17
40	96.2 ± 0.6	75.1 ± 1.1	16.92	3.45	20.37

[a] H_2O: $\gamma_L = 72.80$ mN m^{-1}, $\gamma_L^d = 21.80$ mN m^{-1}, $\gamma_L^p = 51.00$ mN m^{-1} (ref 14f). Ethylene glycol: $\gamma_L = 48.3$ mN m^{-1}, $\gamma_L^d = 29.3$ mN m^{-1}, $\gamma_L^p = 19.0$ mN m^{-1} (ref 14f).

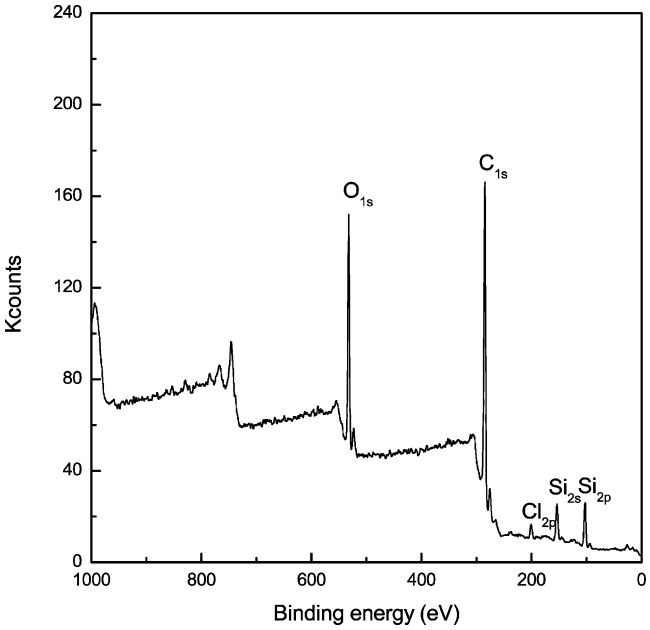

Figure 8. XPS spectrum of the epoxy thermoset containing 10 wt % POSS-capped PCL.

hydrophobilicity of the materials was significantly enhanced; i.e., the surface energy of the materials was reduced. The surface free energies of the hybrid nanocomposites containing different percentage of POSS-capped PCL were calculated according to the geometric mean model:[14a,b]

$$\cos\theta = \frac{2}{\gamma_L}[(\gamma_L^d\gamma_s^d)^{1/2} + (\gamma_L^p\gamma_s^p)^{1/2}] - 1 \quad (4)$$

$$\gamma_s = \gamma_s^d + \gamma_s^p \quad (5)$$

where θ is contact angle and γ_L is the liquid surface tension; γ_L^p and γ_L^d are the polar and dispersive components of γ_L, respectively. According to the data of surface contact angles from water and glycol, the calculated results of surface energy are also incorporated into Table 2. The surface energy of the control epoxy is about 30.4 mN m^{-1}. It is noted that the total surface free energies of the nanocomposites were diminished to 20.4 mN m^{-1} while the concentration of POSS-capped PCL is 40 wt %. The nonpolar component (i.e., γ_s^d) seems to be more sensitive than the polar component (i.e., γ_s^p) to the concentration of the POSS-capped PCL, suggesting that the inclusion of POSS-capped PCL significantly increased the distribution of the nonpolar groups (i.e., silsesquioxane cage) on the surface energy of materials; i.e., the distribution of POSS cages on the surface was increased. The silsesquioxane portion of the organic−inorganic amphiphile on the surface acted as a screening agent to reduce the surface energy of the nanostructured thermosets.[14c,d]

In order to confirm the enrichment of POSS on the surface of the nanostructured thermosets, X-ray photoelectron spectroscopy (XPS) was used to investigate the surface elemental compositions of the nanostructured thermosets containing POSS-capped PCL. Representatively shown in Figure 8 is the XPS spectrum of the nanocomposites containing 10 wt % POSS-capped PCL. The C 1s peak was observed at about 286.8 eV, which was responsible for the contribution of several kinds of carbon atoms from the epoxy thermoset and POSS-capped PCL. The O 1s peak was at ∼535 eV. The Si atoms from silsesquioxane moiety of POSS-capped PCL contributed the Si 2s and Si 2p signals at 156 and 105 eV, respectively. It should be pointed out that the signals of Cl and N are too weak to be shown in this spectrum. The relative concentrations of C, O, N, Cl, and Si on the surfaces of the organic−inorganic hybrid composites, calculated from the corresponding photoelectron peak areas, are listed in Table 3. It is seen that the carbon and oxygen were dominant on the detected surfaces of all the nanostructured thermosets, and a small amount of nitrogen and chlorine from MOCA moiety was also detected. It is noticed that the concentrations of element Si on the surface of the nanostructured thermosets are significantly higher than the theoretical values calculated in terms of feed ratios. The surface Si content increased with increasing POSS-capped PCL in the nanostructured thermosets. For instance, the surface Si content is 10.53 mol % while the concentration of POSS-capped PCL is 30 wt %, and this value is much higher than 1.07 mol % of the theoretical value. This observation suggests that there exists the enrichment of Si-containing moiety on the surfaces of the nanostructured thermosets. This result is important to understand the improvement in surface hydrophobilicity for the nanocomposites. It is worth noticing that the enrichment of Si element on the surfaces of the nanocomposites does not monotonously increase with increasing the concentration of POSS-capped PCL in the thermosets, which could be related to the nanostructures of the thermosets.

Table 3. Elemental Compositions of the Surfaces of the Epoxy Thermosets Containing POSS-Capped PCL Determined by Means of XPS

POSS-capped PCL (wt %)	experimental composition (mol %)					theoretical composition (mol %)				
	C	O	Si	Cl	N	C	O	Si	Cl	N
0	78.00	18.14	0.00	1.56	2.30	83.50	10.86	0.00	2.82	2.82
10	67.54	22.14	7.98	1.24	1.10	82.73	11.69	0.33	2.63	2.63
20	68.95	20.45	8.07	1.23	1.30	81.90	12.57	0.69	2.42	2.42
30	53.70	31.13	10.53	3.29	1.35	81.01	13.53	1.07	2.20	2.20
40	65.90	23.54	8.39	1.26	0.92	80.06	14.55	1.48	1.95	1.95

Conclusions

Polyhedral oligomeric silsesquioxane (POSS)-capped PCL was synthesized via ring-opening polymerization of ϵ-caprolactone with 3-hydroxypropylheptaphenyl POSS as the initiator. The novel organic−inorganic amphiphile was used to incorporate into epoxy resin to prepare the nanostructured thermosets. The nanostructures of the organic−inorganic hybrids were characterized by means of atomic force microscopy (AFM) and transmission electron microscopy (TEM). The formation of the nanostructures in the epoxy thermosets was addressed on the basis of the miscibility and phase behavior of the subcomponents (viz. POSS and PCL chains) of the organic−inorganic amphiphilic macromolecule with epoxy resin after and before curing reaction. It is judged that the formation of the nanostructures in the organic−inorganic hybrid composites follows the mechanism of self-assembly. The static contact angle measurements indicate that the organic−inorganic nanocomposites displayed a significant enhancement in surface hydrophobicity as well as reduction in surface free energy. The improvement in surface properties was ascribed to the enrichment of POSS moiety on the surface of the nanostructured thermosets, which was evidenced by X-ray photoelectron spectroscopy (XPS).

Acknowledgment. The financial support from the Natural Science foundation of China (Project No. 20474038 and 50390090) is acknowledged. S.Z. thanks the Shanghai Educational Development Foundation, China, under an award (2004-SG-18) to the "Shuguang Scholar".

References and Notes

(1) Pascault, J. P.; Williams, R. J. J. In *Polymer Blends*; Paul, D. R., Bucknall, C. B., Eds.; Wiley: New York, 2000; Vol. 1, pp 379−415.

(2) (a) Hillmyer, M. A.; Lipic, P. M.; Hajduk, D. A.; Almdal, K.; Bates, F. S. *J. Am. Chem. Soc.* **1997**, *119*, 2749. (b) Lipic, P. M.; Bates, F. S.; Hillmyer, M. A. *J. Am. Chem. Soc.* **1998**, *120*, 8963.

(3) (a) Mijovic, J.; Shen, M.; Sy, J. W.; Mondragon, I. *Macromolecules* **2000**, *33*, 5235. (b) Grubbs, R. B.; Dean, J. M.; Broz, M. E.; Bates, F. S. *Macromolecules* **2000**, *33*, 9522. (c) Kosonen, H.; Ruokolainen, J.; Nyholm, P.; Ikkala, O. *Macromolecules* **2001**, *34*, 3046. (d) Kosonen, H.; Ruokolainen, J.; Nyholm, P.; Ikkala, O. *Polymer* **2001**, *42*, 9481. (e) Guo, Q.; Thomann, R.; Gronski, W. *Macromolecules* **2002**, *35*, 3133. (f) Ritzenthaler, S.; Court, F.; Girard-Reydet, E.; Leibler, L.; Pascault, J. P. *Macromolecules* **2002**, *35*, 6245. (g) Ritzenthaler, S.; Court, F.; Girard-Reydet, E.; Leibler, L.; Pascault, J. P. *Macromolecules* **2003**, *36*, 118. (h) Guo, Q.; Dean, J. M.; Grubbs, R. B.; Bates, F. S. *J. Polym. Sci., Part B: Polym. Phys.* **2003**, *41*, 1994. (i) Dean, J. M.; Grubbs, R. B.; Saad, W.; Cook, R. F.; Bates, F. S. *J. Polym. Sci., Part B: Polym. Phys.* **2003**, *41*, 2444. (j) Guo, Q.; Thomann, R.; Gronski, W. *Macromolecules* **2003**, *36*, 3635. (k) Dean, J. M.; Verghese, N. E.; Pham, H. Q.; Bates, F. S. *Macromolecules* **2003**, *36*, 9267. (l) Rebizant, V.; Abetz, V.; Tournihac, T.; Court, F.; Leibler, L. *Macromolecules* **2003**, *36*, 9889. (m) Rebizant, V.; Venet, A. S.; Tournillhac, F.; Girard-Reydet, E.; Navarro, C.; Pascault, J. P.; Leibler, L. *Macromolecules* **2004**, *37*, 8017. (n) Wu, J.; Thio, Y. S.; Bates, F. S. *J. Polym. Sci., Part B: Polym. Phys.* **2005**, *43*, 1950.

(4) (a) Larrañaga, M.; Gabilondo, N.; Kortaberria, G.; Serrano, E.; Remiro, P.; Riccardi, C. C.; Mondragon, I. *Polymer* **2005**, *46*, 7082. (b) Meng, F.; Zheng, S.; Zhang, W.; Li, H.; Liang, Q. *Macromolecules* **2006**, *39*, 711. (c) Serrano, E.; Tercjak, A.; Kortaberria, G.; Pomposo, J. A.; Mecerreyes, D.; Zafeiropoulos, N. E.; Stamm, M.; Mondragon, I. *Macromolecules* **2006**, *39*, 2254. (d) Meng, F.; Zheng, S.; Li, H.; Liang, Q.; Liu, T. *Macromolecules* **2006**, *39*, 5072. (e) Meng, F.; Zheng, S.; Liu, T. *Polymer* **2006**, *47*, 7590. (f) Sinturel, C.; Vayer, M.; Erre, R.; Amenitsch, H. *Macromolecules* **2007**, *40*, 2532. (g) Xu, Z.; Zheng, S. *Macromolecules* **2007**, *40*, 2548.

(5) Flory, P. J. *Principles of Polymer Chemistry*; Cornell University Press: Ithaca, NY, 1953.

(6) (a) Lichtenhan, J. D.; Vu, N. Q.; Carter, J. A.; Gilman, J. W.; Feher, F. J. *Macromolecules* **1993**, *26*, 2141. (b) Haddad, T. S.; Lichtenhan, J. D. *J. Inorg. Organomet. Polym.* **1995**, *5*, 237. (c) Lichtenhan, J. D.; Otonari, Y. A.; Carr, M. J. *Macromolecules* **1995**, *28*, 8435. (d) Zhang, C.; Laine, R. M. *J. Organomet. Chem.* **1996**, *521*, 199. (e) Mantz, R. A.; Jones, P. F.; Chaffee, K. P.; Lichtenhan, J. D.; Gilman, J. W.; Ismail, I. M. K.; Burmeister, M. J. *Chem. Mater.* **1996**, *8*, 1250. (f) Haddad, T. S.; Lichtenhan, J. D. *Macromolecules* **1996**, *29*, 7302. (g) Feher, F. J.; Wyndham, K. D.; Baldwin, R. K.; Soulivong, D.; Lichtenhan, J. D.; Ziller, J. W. *Chem. Commun.* **1999**, 1289. (h) Li, G.; Wang, L.; Ni, H.; Pittman, C. U. *J. Inorg. Organomet. Polym.* **2001**, *11*, 123. (i) Abe, Y.; Gunji, T. *Prog. Polym. Sci.* **2004**, *29*, 149. (j) Ni, Y.; Zheng, S. *Chem. Mater.* **2004**, *15*, 5141. (k) Ni, Y.; Zheng, S.; Nie, K. *Polymer* **2004**, *45*, 5557. (l) Chan, S.-C.; Kuo, S.-W.; Chang, F.-C. *Macromolecules* **2005**, *38*, 3099. (m) Wadon, A. J.; Zheng, L.; Farris, R. J.; Coughlin, E. B. *Macromolecules* **2001**, *34*, 8034.

(7) (a) Lee, A.; Lichtenhan, J. D. *Macromolecules* **1998**, *31*, 4970. (b) Choi, J.; Harcup, J.; Yee, A. F.; Zhu, Q.; Laine, R. M. *J. Am. Chem. Sci.* **2001**, *123*, 11420. (c) Choi, J.; Kim, S. G.; Laine, R. M. *Macromolecules* **2004**, *37*, 99. (d) Laine, R. M.; Choi, J.; Lee, I. *Adv. Mater.* **2001**, *13*, 800. (e) Choi, J.; Yee, A. F.; Laine, R. M. *Macromolecules* **2003**, *36*, 5666. (f) Choi, J.; Tamaki, R.; Kim, S. G.; Laine, R. M. *Chem. Mater.* **2003**, *15*, 3365. (g) Choi, J.; Yee, A. F.; Laine, R. M. *Macromolecules* **2004**, *37*, 3267. (h) Abad, M. J.; Barral, L.; Fasce, D. F.; Williams, R. J. J. *Macromolecules* **2003**, *36*, 3128. (i) Zucchi, I. A.; Galante, M. J.; WilliamsR, J. J.; Franchini, E.; Galy, J.; Gerard, J.-F. *Macromolecules* **2007**, *40*, 1274. (j) Liu, H.; Zheng, S.; Nie, K. *Macromolecules* **2005**, *38*, 5088. (k) Matejka, L.; Strachota, A.; Plestil, J.; Whelan, P.; Steinhart, M.; Slouf, M. *Macromolecules* **2004**, *37*, 9449. (l) Strachota, A.; Kroutilova, I.; Kovarova, J.; Matejka, L. *Macromolecules* **2004**, *38*, 9457.

(8) (a) Yin, M.; Zheng, S. *Macromol. Chem. Phys.* **2005**, *206*, 929. (b) Ni, Y.; Zheng, S. *Polymer* **2005**, *46*, 5828.

(9) (a) Brown, J. F., Jr.; Vogt, L. H., Jr.; Prescott, P. I. *J. Am. Chem. Soc.* **1964**, *86*, 1120. (b) Ni, Y.; Zheng, S. *J. Polym. Sci., Part A: Polym. Chem.* **2007**, *45*, 1247. (c) Ni, Y.; Zheng, S. *J. Polym. Sci., Part B: Polym. Phys.* **2007**, *45*, 2201. (d) Wadon, A. J.; Coughlin, E. B. *Chem. Mater.* **2003**, *15*, 4555.

(10) (a) Schmitz, I.; Schreiner, M.; Friedbacher, G.; Grasserbauer, M. *Appl. Surf. Sci.* **1997**, *115*, 190. (b) Magonov, S. N.; Elings, V.; Whangbo, M. H. *Surf. Sci.* **1997**, *375*, L385. (c) Tamayo, A.; Garcia, R. *Langmuir* **1996**, *12*, 4434. (d) Chen, X.; McGurk, S. L.; Davies, M. C.; Roberts, C. J.; Shakesheff, K. M.; Davies, J.; Dawkes Domb, A. *Macromolecules* **1998**, *31*, 2278. (e) Clarke, S.; Davies, M. C.; Roberts, C. J.; Tendler, S. J. B.; Williams, P. M.; Lewis, A. L.; O'Bryrne, V. *Macromolecules* **2001**, *34*, 4166.

(11) Nojima, S.; Hashizume, K.; Rohadi, A.; Sasaki, S. *Polymer* **1997**, *38*, 2711.

(12) (a) Fox, T. G. *Bull. Am. Phys. Soc.* **1956**, *1*, 123. (b) Gordon, M.; Taylor, J. S. *J. Appl. Chem.* **1952**, *2*, 496. (c) Couchman, P. R. *Macromolecules* **1978**, *11*, 1156.

(13) (a) Coleman, M. M.; Painter, P. C. *Prog. Polym. Sci.* **1995**, *20*, 1. (b) Coleman, M. M.; Graf, J. F.; Painter, P. C. *Specific Interactions and the Miscibility of Polymer Blends*; Technomic Publishing: Lancaster, PA, 1991.

(14) (a) Kaelble, D. H.; Uy, K. C. *J. Adhes.* **1970**, *2*, 50. (b) Kaelble, D. H. *Physical Chemistry of Adhesion*; Wiley-Interscience: New York, 1971. (c) Turri, S.; Levi, M. *Macromolecules* **2005**, *38*, 5569. (d) Turri, S.; Levi, M. *Macromol. Rapid Commun.* **2005**, *26*, 1233. (e) Koh, K.; Sugiyama, S.; Morinaga, T.; Ohno, K.; Tsujii, Y.; Fukuda, T.; Yamahiro, M.; Iijima, T.; Oikawa, H.; Watanabe, K.; Miyashita, T. *Macromolecules* **2005**, *38*, 1264. (f) Adamson, A. W. *Physical Chemistry of Surfaces*, 5th ed.; Wiley-Interscience: New York, 1990.

MA0709351